

Supporting Information

Kinetic Analysis of the M2 Proton Conduction of the Influenza Virus

Rafal M. Pielak and James J. Chou

*Department of Biological Chemistry and Molecular Pharmacology, Harvard Medical School,
Boston, Massachusetts 02115 and Program in Biological and Biomedical Sciences, Harvard
Medical School, Boston, Massachusetts 02115*

RECEIVED DATE (automatically inserted by publisher); E-mail: chou@cmcd.hms.harvard.edu

Protein expression, purification, and labeling

M2₁₈₋₆₀ and its variants are cloned, expressed and purified as previously described¹. Briefly, the protein was expressed into inclusion bodies as a fusion to His9–trpLE. The M2₁₈₋₆₀ peptide was released from the fusion protein by cyanogen bromide digestion in 70% formic acid (1 hr, 0.2 g/ml cyanogen bromide, 70% formic acid). The digest was dialyzed against water, lyophilized, and loaded onto a C4 column (Grace–Vydac) in 2:1:2 hexafluoroisopropanol:formic acid:water and separated using a gradient of 3:2 isopropanol:acetonitrile. For selective ¹³C-labeling of histidine, 100 mg/L of ¹³C₆, ¹⁵N₃ labeled L-histidine (Isotec, Sigma) was added 1 hr before induction with IPTG. The lyophilized peptide was then refolded at 250 mM by dissolving in 6 M guanidine and 150 mM DHPC and dialyzing against the final NMR buffer containing 40 mM sodium phosphate and 30 mM glutamate. The sample was concentrated to a final concentration of 0.75 mM (monomer). Rimantadine was added after concentrating. The concentration of DHPC was determined from ¹H NMR spectroscopy to be around 300 mM.

Liposomal proton flux assay

Liposome assay for M2 channels was established based on works from the Schroeder, Miller and Busath labs²⁻⁴. In this assay, a proton gradient was used to drive proton conduction. Liposomes were made with identical pH and ion concentrations inside and outside, but highly buffered inside and only weakly buffered outside. Protein-mediated conductance of protons from the external bath into the liposome interior was initiated by adding hydrochloric acid under continuous rapid mixing. Proton flux was monitored as an increase in pH of the external bath.

M2₁₈₋₆₀ channels were reconstituted into liposomes by mixing 10 mg of *E. coli* polar lipid extract (Avanti Polar Lipids), 2.5, 5, or 10 nmols of M2₁₈₋₆₀ peptide, and 0.2 nmol of the potassium ionophore valinomycin in 1.1 mL of a 2:1 mixture of chloroform and methanol. The solution was dried down to thin films under nitrogen gas. The films

were redissolved in 750 μL of chloroform and dried down a second time under nitrogen resulting in high-quality, transparent thin films. Liposomes were then formed by resuspending the thin films in strongly-buffered internal liposome buffer (50 mM phosphate, 50 mM citrate, 122 mM KCl, 122 mM NaCl, 0.01% NaN_3 , pH 7.7), and extruding 15 times through 0.2 μM polycarbonate membranes. The external buffer was exchanged by running 750 μL of the liposome solution over a PD-10 column (GE Health Sciences) pre-equilibrated with weakly-buffered external vesicle buffer (EVB: 2 mM phosphate, 2 mM citrate, 122 mM KCl, 122 mM NaCl, 0.01% NaN_3 , pH 7.8); eluted volume was 1.5 mL. Then, multiple samples, prepared as described above, were combined together (reduce variability between individual samples) and split into 1 ml final samples containing ~ 5 mg/mL lipid, 1.5, 3, or 6 μM M2₁₈₋₆₀ peptide, and 0.1 μM valinomycin. Valinomycin in small quantities was required to allow potassium ions to flow across the membrane in the opposite direction of protons to avoid generating a charge potential. No proton conductance was observed in the absence of valinomycin. The liposomes had diameters of ~ 160 nm, as determined by dynamic light scattering. From this, we estimate that there are ~ 15 , 30, or 60 channels per liposome, 50% of which, it is assumed, have the correct orientation to conduct protons into the liposome⁵. Initial pH inside and outside of liposomes was identical. Protein-mediated conductance of protons from the bath into the liposomes was initiated by lowering the external pH by addition of 1 M HCl with continuous rapid mixing with a micro-stir bar. Proton flux was monitored as an increase in pH of the external bath with a pH micro-electrode (InLab). Reported flux rates were taken as the average rate observed over the period from 15 to 24 seconds after the addition of HCl. The assay was terminated by the addition of 5 μM of the proton ionophore carbonylcyanide-4-trifluoromethoxyphenylhydrazone (FCCP). The effects of buffering from citrate, phosphate, rimantadine, and lipids was evaluated by addition of 5, 10, or 15 μL of 50 mM HCl. Since the proton fluxes are taken as the initial change in pH, a correction factor was required to account for the increased buffering capacity of the solution after the system was uncoupled by FCCP. The excess buffering from the uncoupled liposome interiors was determined in a series of peptide-free controls containing 4.7, 5.0, or 5.3 mg/mL of lipid by adding 5 μL of 50 mM HCl before and after addition of FCCP. The excess buffering capacity of the external buffer was found to be 12 \pm 2% that of the FCCP uncoupled system. To assay channel inhibition, rimantadine

was added from concentrated stock solutions in anhydrous ethanol (Sigma) five minutes before initiation of proton flux.

Initial rates of proton fluxes measured at different initial pH values were plotted and fit to Eq. 1 using MATLAB.

NMR pH titration of Trp41 indole amine

A series of 2D TROSY spectra for WT at different pH values from 8 - 5 were recorded at 600 MHz (^1H frequency). The changes in chemical shift (sum of ^1H and ^{15}N shifts) for the Trp41 indole amine at various pH points were plotted and the curve was fit using MATLAB to the Hill equation: $f(x) = a / (1 + 10^{h(x-pK)})$; $x = \text{pH}$.

NMR pH titration of His37 imidazole

A series of ^{13}C 1D spectra of the double mutant (E56K, H57Y) of M2₁₈₋₆₀ with only His37 ^{13}C labeled were recorded at different pH values (7.3 – 5) using direct carbon detection (^{13}C frequency 125 MHz). The changes in peak height vs. pH for the His37 $^{13}\text{C}_{\epsilon 1}$ were plotted and fit as above for Trp41.

k_{trans} and K_{app} equations derived based on the reaction scheme 2.

$$k_{\text{trans}} = \frac{k_1 k_3}{(k_1 + k_3)}$$

$$K_{\text{app}} = \frac{(k_1 + k_{-1})(k_{-2} + k_3)}{(k_1 k_2 + k_2 k_3)}$$

Assuming that $k_3 \ll k_{-2}$

$$K_{\text{app}} \approx (k_{-2}/k_2) [(k_1 + k_{-1}) / (k_1 + k_3)]$$

or equivalently,

$$\text{p}K_{\text{app}} \approx \left\{ -\log(k_{-2}/k_2) \right\} + \left\{ -\log[(k_1 + k_{-1}) / (k_1 + k_3)] \right\}$$

1. Schnell, J.R. & Chou, J.J. Structure and mechanism of the M2 proton channel of influenza A virus. *Nature* **451**, 591-5 (2008).
2. Schroeder, C., Ford, C.M., Wharton, S.A. & Hay, A.J. Functional reconstitution in lipid vesicles of influenza virus M2 protein expressed by baculovirus: evidence for proton transfer activity. *J Gen Virol* **75 (Pt 12)**, 3477-84 (1994).
3. Nguitrageol, W. & Miller, C. Uncoupling of a CLC Cl⁻/H⁺ exchange transporter by polyatomic anions. *J Mol Biol* **362**, 682-90 (2006).
4. Moffat, J.C. et al. Proton transport through influenza A virus M2 protein reconstituted in vesicles. *Biophys J* **94**, 434-45 (2008).
5. Lin, T.I. & Schroeder, C. Definitive assignment of proton selectivity and attoampere unitary current to the M2 ion channel protein of influenza A virus. *J Virol* **75**, 3647-56 (2001).

Supplementary Table 1 Proton transport rates of M2₁₈₋₆₀ and its variants ¹

	k_{trans} (H ⁺ s ⁻¹)	σ ²	K_{app} (M)	σ ²	$\text{p}K_{\text{app}}$ ³	n ⁴
WT	14.0	0.5	5.66 x10 ⁻⁷	1.15 x10 ⁻⁷	6.25	3
WT (pH 5-3)	40.0	4.5	1.88 x10 ⁻⁵	4.24 x10 ⁻⁷	4.73	2
V27A	30.1	1.4	5.05 x10 ⁻⁷	1.75 x10 ⁻⁷	6.30	2
S31A	8.62	0.16	2.95 x10 ⁻⁷	1.98 x10 ⁻⁹	6.53	2
D44A	7.46		7.72 x10 ⁻⁷		6.11	1

¹ The pH range for the measurements is ~7 – 5 unless labeled otherwise. The values are averaged over number of samples.

² σ is the standard deviation.

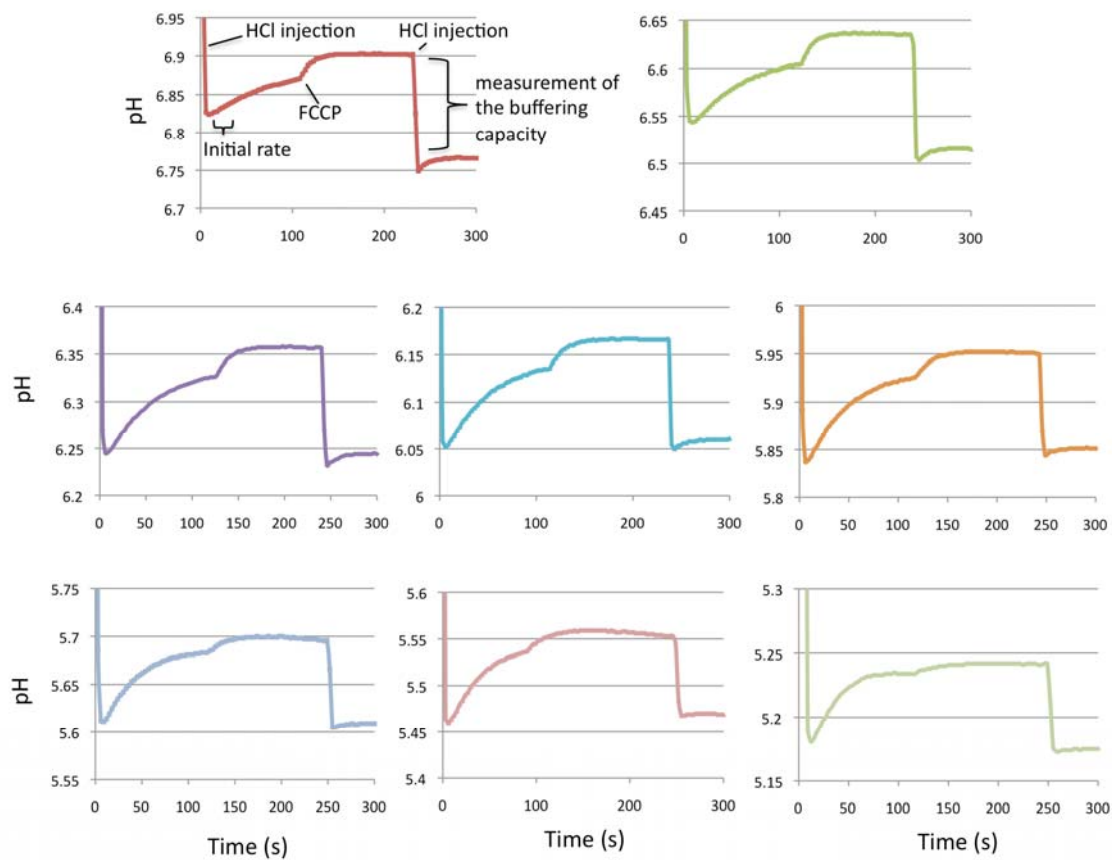
³ $\text{p}K_{\text{app}} = -\log_{10}(K_{\text{app}})$.

⁴ n represents the number of times the entire saturation curve was repeated (the number of points per curve was between 7 and 10 except for WT (pH 5-3) where the number of points per curve was 5).

Supplementary Table 2 Fitting statistics for representative conductance curves presented in **Fig. 1a&b** and **Fig. 3**.

	k_{trans} (H ⁺ s ⁻¹)	K_{app} (M)	$\text{p}K_{\text{app}}$	R-square	RMSE ¹
WT	13.59	5.69 x10 ⁻⁷	6.24	0.978	0.591
WT (pH 5-3)	43.48	1.91 x10 ⁻⁵	4.72	0.974	1.850
V27A	29.85	4.79 x10 ⁻⁷	6.32	0.963	1.512
S31A	8.75	3.00 x10 ⁻⁷	6.52	0.978	0.323
D44A	7.46	7.72 x10 ⁻⁷	6.11	0.985	0.286

¹ RMSE - root mean square error



Supplementary Figure 1. Representative traces of WT M2₁₈₋₆₀ proton conductance at different starting pH values. Each panel represents single experiment at different starting pH value. Protein-mediated protons flux from the external bath into the liposome interior was initiated by adding hydrochloric acid (HCl) under continuous rapid mixing. Proton flux was monitored as an increase in pH of the external bath. The flux rates were taken as the average rate observed over the period from 15 to 24 seconds after the addition of HCl. The assay was terminated by the addition of 5 μ M of the proton ionophore carbonylcyanide-4-trifluoromethoxyphenylhydrazone (FCCP). The effects of buffering from citrate, phosphate, and lipids were evaluated by addition of 5 μ L of 50 mM HCl. The initial rates of proton flux at different starting pH values were then used for kinetics analysis (**Fig. 1**).